

PDF hosted at the Radboud Repository of the Radboud University Nijmegen

The following full text is a publisher's version.

For additional information about this publication click this link.

<http://hdl.handle.net/2066/104038>

Please be advised that this information was generated on 2017-12-06 and may be subject to change.

Strained semiconductor clusters in sodalite

F. Buda

Scheikundig Laboratorium der Vrije Universiteit, De Boelelaan 1083, 1081 HV Amsterdam, The Netherlands

A. Fasolino

*Research Institute for Materials, Institute of Theoretical Physics, University of Nijmegen, Toernooiveld,
NL-6525ED Nijmegen, The Netherlands*

(Received 16 March 1999)

We have studied, by the *ab initio* Car-Parrinello molecular-dynamics approach, the structure and band gaps of III-V semiconductor clusters included in sodalite as a function of the cluster size up to full filling of the sodalite cage. This study allows us to address directly the role of quantum confinement. The minimum-energy structures present large deviations from bulklike tetrahedral coordination and are reminiscent of amorphous structures. In contrast to the quantum confinement picture, the energy gap grows for increasing cluster size. The shift of the gap is instead due to an effective tensile/compressive strain exerted by the cage on the cluster and is comparable to the variation of the bulk band gap under the effect of hydrostatic pressure.

[S0163-1829(99)12931-X]

I. INTRODUCTION

Modern electronics is largely based on quasi-two-dimensional semiconductor structures (quantum wells, heterostructures). Much effort is currently devoted to achieve confinement in more than one direction (quantum wires, dots) in a controllable fashion.

One recent trend is to achieve this goal by means of self-organizing processes.¹ One promising strategy, which is being actively experimentally explored for different types of applications,^{2–10} is the growth of semiconductor into materials, such as the zeolites, which present cavities of well-defined dimensions that serve as natural templates for the growth of clusters and wires. This procedure would have the enormous advantage of not being dependent on suitable and often expensive substrates, a problem particularly serious for GaN-based structures. On the other hand, it is important to realize that, contrary to the case of epitaxial growth, the equilibrium structure of clusters encapsulated in zeolites is not necessarily bulklike. Consequently, the electronic properties cannot be *a priori* calculated by imposing appropriate boundary conditions to the Hamiltonian describing the bulk electronic structure. The concept of quantum confinement, namely, the increasing of the gap in spatially confined semiconductors, derives in fact by such an approach where the properties of a thin layer (wire, dot) embedded in a material with larger band gap are calculated as the bound states in an effective confining potential in analogy to the particle in a box quantum-mechanical model. For semiconductor clusters in host lattices, the crucial question that has to be answered before proceeding to calculate the electronic properties is whether bulklike bonding will be preserved after encapsulation so that the interaction of the cluster with the zeolite framework can be represented by an effective confining potential.

The *ab initio* Car-Parrinello molecular dynamics¹¹ (AIMD) is the ideal technique for this purpose because it allows us to calculate the electronic properties after a full

structural optimization has been performed by means of a simulated annealing. In this paper, we present an AIMD study of the structural stability and electronic properties of small (4–10 atoms) III-V clusters in interaction with the sodalite cage (III-V/SOD from now on) as a function of the filling of the cage. Isolated hydrogen saturated III-V microclusters,¹² the natural sodalite,¹³ and smaller III-V/SOD (Ref. 14) and II-VI/SOD (Ref. 15) clusters in the sodalite crystal, have recently been studied within this theoretical approach. Demkov and Sankey have performed, by an approach similar to ours, an interesting related study of Si microclusters in all-silica sodalite.¹⁶ The same group has also recently studied the electronic structure of black sodalite.¹⁷ We note that most experimental work deals with zeolites with much larger unit cells. Conversely the sodalite structure, with 36 atoms in the unit cell, allows detailed *ab initio* theoretical studies and is taking a prototype role for the understanding of the interactions in the composite cluster-zeolite materials. Here we focus on the size dependence of the electronic gap for a given III-V compound, thus addressing directly the role of quantum confinement. The present work generalizes the conclusions of our previous study of III₄V₁/SOD clusters of several III-V materials.¹⁴

We anticipate here our most important results concerning the structure and electronic states:

The structure of the embedded clusters presents large deviations from tetrahedral coordination, with anion-anion and cation-cation bonding and two-, three-, and fourfold coordination. One common feature is that the III and V atoms are organized, roughly speaking, in two shells leaving the center of the cage empty: the inner shell is composed of cation and anion atoms, the outer one of cation (Ga) atoms bonded to the oxygen atoms of the cage.

Contrary to the expectations of quantum confinement, the highest occupied molecular orbital–lowest unoccupied molecular orbital (HOMO-LUMO) gap increases in going to larger clusters. A substantial energy shift is instead caused by an effective tensile/compressive strain induced by the cage

and displays a behavior similar to that of the bulk band gap in the presence of a hydrostatic pressure.

The paper is organized as follows. In Sec. II we give some technical details about the physical system and computational approach. In Sec. III we present the results for the structure and energy gaps. In this section we also discuss some relevant experimental results. Finally, we conclude in Sec. IV with some general remarks and perspectives.

II. PHYSICAL SYSTEM AND COMPUTATIONAL APPROACH

In the AIMD simulations, the forces on the atoms are computed using the density-functional theory¹⁸ for the electronic structure. We treat explicitly the valence electrons only and use pseudopotentials to describe the interaction with the frozen-core electrons. In particular, we use first-principle soft pseudopotentials¹⁹ for the first-row elements (O and N) and norm-conserving pseudopotentials²⁰ for the other elements. The chosen energy cutoff of 20 Ry for the plane-wave expansion of the Kohn-Sham orbitals ensures a good convergence of the results. In particular, we have checked that an increase of the cut-off from 20 to 25 Ry results in negligible changes of the structural properties of natural sodalite.¹³ The electronic properties are calculated only at the Brillouin-zone center Γ , which in view of the large unit cell of the sodalite should yield a good description of the electronic charge density. The favorable comparison of the structural parameters and of the electronic density of states calculated within this approximation with the experimental data for natural sodalite¹³ supports this assumption. The exchange-correlation functional is treated within the local density approximation (LDA). It is well known that the LDA strongly underestimates the energy gap for semiconductor materials. However, it is reliable in reproducing general trends as functions of size and composition. Generalized gradient corrections (GGA) to LDA were not included in the present calculation since the LDA accurately describes the structure of strong covalent bonded systems, as the ones studied in this work. Moreover, the GGA do not significantly improve the LDA underestimation of the energy gap in semiconductors that is of interest here.²¹

We use the unitary cell of aluminosilicalite sodalite $\text{Si}_6\text{Al}_6\text{O}_{24}$ (Ref. 22) (SOD) with periodic boundary conditions to represent the full crystal. We take throughout the lattice parameter of natural sodalite as determined within the LDA $a = 8.92 \text{ \AA}$ (Ref. 13) instead of the experimental value $a = 8.882 \text{ \AA}$.²² Aluminosilicalite sodalite is not inert as the silicasodalite ($\text{Si}_{12}\text{O}_{24}$) because the presence of six Al per unit cell causes a deficiency of three electrons per cage, which is compensated in natural sodalite by one Na_4Cl cluster per cage.¹³ The volume of the unit cell is twice the volume of the sodalite cage, so that we can choose to fill either each cage with one cluster (filling factor 1) or every two cages with one cluster (filling factor $\frac{1}{2}$). For III-V clusters with more than five atoms, we have chosen half-filling so that only every second cage is occupied by a cluster. This choice is motivated by the fact that we want to ascertain whether addition of atoms leads to larger clusters, possibly with bulklike coordination, or to fragmentation of the clusters going to occupy both cages in the unit cell. In addition,

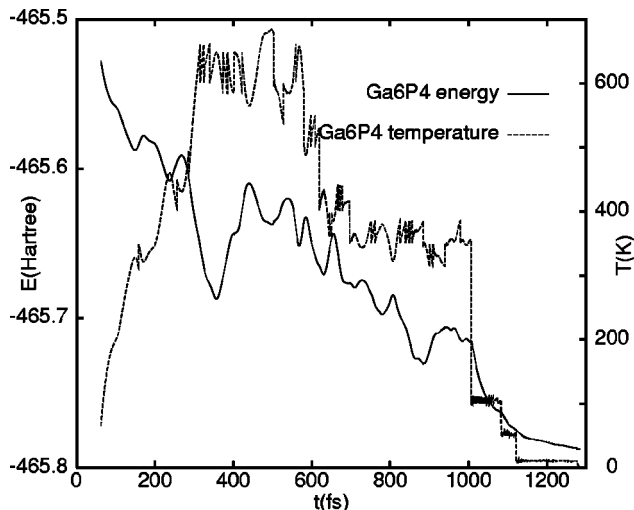


FIG. 1. Temperature (dashed line) and total energy (solid line) along the simulated annealing of the largest cluster studied Ga_6P_4 . Notice the rather unusual deep local minima along the path.

half-filling suppresses cluster-cluster interactions. We have studied GaP and GaN clusters with four, five, and six Ga atoms and one and four P or N atoms. The search for the most stable geometry of the III-V/SOD composite is performed using a simulated annealing approach,¹¹ which allows us to overcome local minima in the potential-energy surface. A typical total simulation time for each cluster is about 1 ps. The so-called mass preconditioning scheme²³ with 5 Ry cutoff for the energy dependent mass has allowed us to use an integration time step of 8 a.u. ($1 \text{ a.u.} = 2.42 \times 10^{-17} \text{ sec}$) while still ensuring adiabatic motion of the ionic degrees of freedom. In particular up to this value we have not observed any drifting of the total energy of the system.

III. RESULTS

A. Ground-state geometry

In a previous work we have shown that for Ga_4P and Ga_4P_4 clusters in sodalite the alternated tetrahedral bulk structure was lost; only group-III atoms were bonded to the oxygen in the cage, leading to segregation of group-V atoms in the interior of the cage.¹⁴ Here we want to study whether addition of more atoms to the cluster up to full filling of the sodalite cage can reestablish an alternating bulklike arrangement. To this purpose, we have considered the following cases:

$\text{Ga}_5\text{P}_4 + \text{Ga}$: the initial configuration of this cluster has been generated by adding an extra Ga atom at the center of the previously studied Ga_4P_4 cluster. At the same time we have added also a Ga atom at the center of the empty adjacent cage in order to have an even number of electrons and to be able to compare the total energy to the Ga_6P_4 case described below. This is why we will refer to this cluster as $\text{Ga}_5\text{P}_4 + \text{Ga}$.

Ga_6P_4 : the initial configuration of this cluster has been generated by adding two extra Ga atoms around the center of the Ga_4P_4 cluster. We have considered also a Ga_6N_4 cluster.

In Fig. 1 we show the temperature and the potential-energy profile during the simulated annealing for the Ga_6P_4

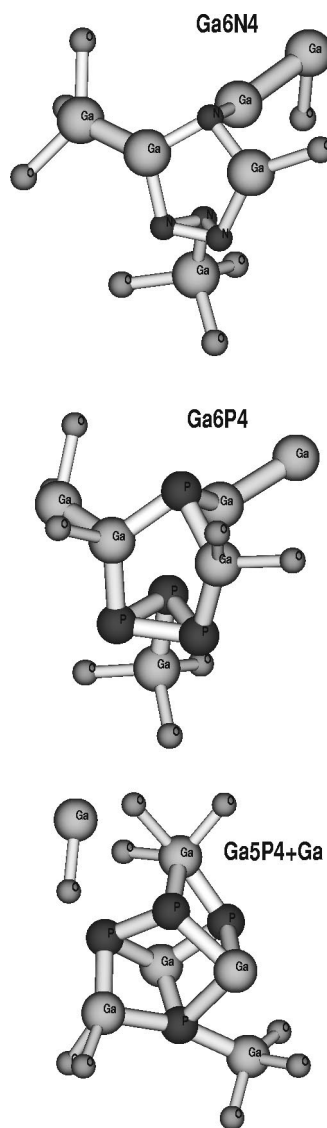


FIG. 2. Structure of the clusters after the simulated annealing. For clarity, instead of the full sodalite cage, we show only the oxygen atoms bonded to the clusters. (a) Ga_6N_4 , (b) Ga_6P_4 , and (c) $\text{Ga}_5\text{P}_4+\text{Ga}$. The Ga atom located in the neighboring cage for case (c) is also shown. Bonds are drawn according to the criterion that the bond length has to be less than the sum of the covalent radii plus 10%.

cluster in sodalite. The evolution to the minimum occurs via a number of metastable states as indicated by the deep local minima in the energy.

The structures after the simulated annealing are shown in Fig. 2. For the sake of clarity, we have shown only the atoms of the cluster and the oxygen atoms of the cage that are bonded to the cluster. The common features are (i) bonding to oxygen occurs via an outer shell of Ga atoms, (ii) many homopolar bonds are present, (iii) a pentagonal structure with anion basis and apex is formed, and (iv) the clusters remain compact.

It is remarkable that the structure of Ga_6P_4 and Ga_6N_4 clusters are very similar despite the very different dimensions of P and N atoms. The calculated structures are very stable even at very high temperatures. Once the minimum-energy structure has been reached, further simulations of the

system at high temperatures (≈ 800 K) just show vibrations around equilibrium positions and no further structural modifications. Some more comments on the structure of $\text{Ga}_5\text{P}_4+\text{Ga}$ are in order: during the simulation, the Ga atom in the empty cage moves away from the initial position at the center of the cage to form a bond with an oxygen atom (shown in Fig. 2). The resulting structure has an energy 1.6 eV higher than that of Ga_6P_4 . In addition to the pentagonal ring, there are square faces that occur also in metastable states of the Ga_6P_4 . This type of arrangement bears a relationship with the results obtained for hydrogenated III-V clusters: for fully hydrogen-saturated clusters, only small distortions with respect to the bulk tetrahedral order take place, whereas when the dangling bonds at the surface of the cluster are only partially hydrogen-saturated, major rearrangements occur, with the formation of square and pentagonal faces [see Fig. 1(c) of Ref. 12]. This result, as well as the presence of homopolar bonding, points out the importance of dangling-bond passivation to preserve the bulklike structure as is also the case at semiconductor surfaces.²⁴ In Fig. 2, we can observe the presence of many undercoordinated atoms (mostly threefold coordinated) and also one fivefold coordinated Ga atom. Only few of the Ga atoms bonded to the cage show a fourfold tetrahedral coordination. The large number of coordination ‘‘defects’’ and the high disorder in the bond angle distribution (with angles ranging from 60° to 160°) are typical features of amorphous materials. This result is in line with a recent report on Se nanoclusters incorporated in the supercages of zeolite Y, where disordered structures similar to amorphous selenium have been observed.⁸

The disorder in the bonding coordination, however, obscures the fact that the structure of the clusters is definitely influenced by the symmetry of the surrounding cage. Remarkably, for the case of Ga_4P_4 , we find that the final equilibrium positions of the Ga atoms are close to the $8e(x,x,x)$ special positions of the $P\bar{4}3n$ group, which are occupied by the Na atoms in natural sodalite. The positions for the cases shown in Fig. 2 are not easily classified according to the structure of the $P\bar{4}3n$ group, although visual inspection of the clusters in the cage suggests a higher degree of order than by looking at the isolated cluster. In particular, the most apparent feature that relates the positions of the atoms in the cluster to the cage is their radial distribution around the center of the cage, which is shown in Fig. 3. We can clearly see that, in all cases, the center of the cage is empty and the clusters are organized in two shells of atoms, the inner composed of anions (P or N), the outer shell composed of cations (Ga) with some overlap between the two. It is interesting to notice that in the ten-atom clusters one of the Ga atoms has ended up just outside the cage rather than occupying the center. This fact, on the one hand, supports our previous speculation¹⁴ that the growth inside the cage is likely to stop after the formation of a bilayer of cations and anions, and, on the other hand, suggests that the cage cannot be further filled.

The average Ga-P bond distances given in Table I show values ranging from smaller to larger than the bulk value. This result has important implications on the electronic properties of these clusters as we will discuss in the next section.

We close the discussion of the structural properties by noting that large rearrangements occur only for the included

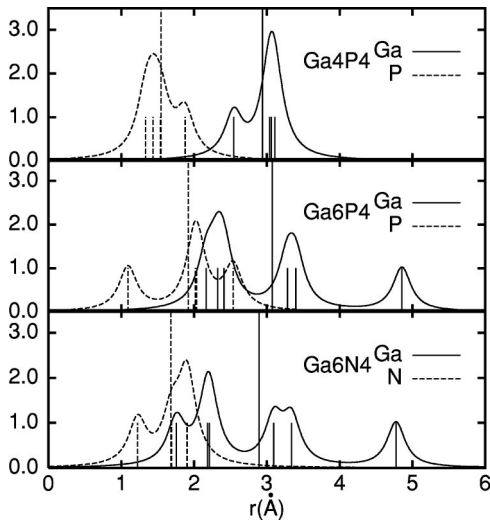


FIG. 3. Distance of the atoms of the cluster from the center of the cage of radius 4.45 Å. We show vertical bars at the actual distances of the final configuration and their envelope when broadened with a Lorentzian of width 0.15 Å, meant to mimic a thermal distribution. (a) Ga_4P_4 , (b) Ga_6P_4 , and (c) Ga_6N_4 . Notice that the cluster is organized in shells, the outer being formed only by Ga cation atoms situated close to the cage. We have shown as vertical lines also the average anion and cation shell radii. Notice also the similarity of the structure of Ga_6P_4 and Ga_6N_4 , despite the different sizes of the anions.

clusters, while the structural parameters of the cage are only slightly affected. In particular, Si and Al atoms remain within 1% of the crystallographic positions.

B. Electronic properties

In this section we will focus on the influence of the cluster size on the resulting energy gap in the context of the quantum confinement model. In Ref. 14 we have shown that the encapsulated clusters introduce a number of electronic states in the large energy gap of the zeolite, resulting in a semiconductor material. The HOMO-LUMO gap for $\text{III}_4\text{V}_1/\text{SOD}$ clusters was found to have a direct relation to that of the corresponding bulk material and much smaller than expected on the basis of quantum confinement in nanometer size dots. Within the local density approximation (which underestimates the energy gap), we found values of ≈ 0.4 eV, ≈ 1.35 eV, and ≈ 1.9 eV for InAs, GaP, and GaN clusters of the same size.

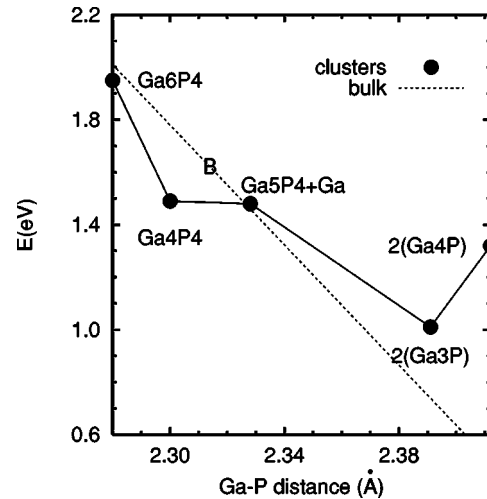


FIG. 4. Calculated energy gap of the indicated clusters included in the sodalite cage as a function of the average cation-anion distance. The solid line connecting the points is a guide to the eye. The dashed line indicates the change of the bulk energy gap as a function of the first-neighbor distance as due to the effect of hydrostatic pressure (Ref. 25). On this line, *B* indicates the value 1.62 eV of the indirect band gap obtained at zero pressure within the local density approximation at the *X* point of the Brillouin zone (the LDA estimate is about 30% lower than the experimental value 2.32 eV).

Ingoing from four-atom to ten-atom clusters, we find that, contrary to the expectations of quantum confinement, the band gap increases. This is illustrated in Fig. 4 where we plot the calculated band gap as a function of the average cation-anion distance. We can clearly see that the HOMO-LUMO gap is substantially blueshifted for the largest clusters and redshifted for the smallest. This behavior is opposite to the prediction of quantum confinement. As shown in Table I, the largest clusters have smaller cation-anion distances than in the bulk, whereas the smallest clusters have larger distances than in the bulk. Therefore, we have interpreted the increase (decrease) of the band gap with respect to the bulk value as due to an effective compressive (tensile) strain induced by the cage. For the largest clusters the strain is not as big as to cause fragmentation but leads to compressed bonds as in the presence of a hydrostatic pressure. This interpretation is confirmed by the comparison of the known dependence of the bulk band gap on hydrostatic pressure²⁵ (dashed line in Fig. 4) with the numerical results obtained for the clusters.

In most experimental studies a blueshift in the absorption spectra has been attributed to quantum confinement,^{3,4} while

TABLE I. Average bond distances within the Ga-P clusters in sodalite. The numbers in parentheses indicate the number of bonds that are considered in the average. The notation $2(\text{Ga}_n\text{P})$ means that each sodalite cage is filled with a Ga_nP cluster (filling factor 1). The bulk Ga-P distance is 2.314 Å within the LDA (experimental value, 2.36 Å).

	$2(\text{Ga}_4\text{P})$	$2(\text{Ga}_3\text{P})$	Ga_4P_4	Ga_6P_4	$\text{Ga}_5\text{P}_4 + \text{Ga}$
Ga-P aver. (Å)	2.412 (6)	2.391 (6)	2.300 (4)	2.280 (6)	2.328 (11)
P-P aver. (Å)			2.241 (4)	2.189 (3)	2.169, 2.385
Ga-O aver. (Å)	2.096 (9)	2.094 (11)	2.057 (9)	2.078 (10)	2.034 (9)
Ga-Ga (Å)				2.291, 2.607	

a large blueshift can also result from strain. Only a direct analysis of the size dependence, difficult to perform experimentally, can distinguish between the two mechanisms. Interestingly, the dependence of the absorption spectra of Cd-S clusters in zeolites with different channel/cage sizes⁶ has been interpreted in terms of mechanical compression/expansion of the bonds, i.e., an effective strain.

A similar reduction of the HOMO-LUMO gap in Si_n (with $n > 5$) clusters in sodalite has also been interpreted as due to an effective pressure in Ref. 16. In all-silica sodalite, where there is no charge transfer between the cluster and the cage, it is possible to compare the HOMO-LUMO gap of the cluster inside the cage and in the vacuum. This has been done in Refs. 16 and 15 for Si and CdS clusters, respectively. The results of these types of comparisons have also been discussed in terms of quantum confinement, but it is difficult to draw definitive conclusions since they depend on a detailed balance of electrostatic and structural effects.^{16,15}

A study of the dependence of the HOMO-LUMO gap on the cluster size as the one we have presented here is, in principle, a more direct way to address the question of the existence of quantum confinement. Our results rule out quantum confinement effects for the growth of III-V clusters in pores of zeolite of the order of 10 Å; the interaction with the cage is so strong that the effect on the semiconductor cluster cannot, even schematically, be described as an effective potential barrier as in the case of quantum dots.

IV. CONCLUSIONS

We have studied by AIMD the structure and electronic properties of III-V semiconductor clusters included in the sodalite cage as a function of cage filling. The structure of

the clusters is clearly determined by the interaction with the zeolite cage, leading to large deviations from the bulklike tetrahedral bonding and to shells of cations and anions leaving the center of the cage empty.

The dependence of the HOMO-LUMO gap of the III-V/SOD composite on the cluster size is opposite to that expected on the basis of the quantum confinement model, increasing ingoing to larger clusters. This behavior is attributed to an effective tensile or compressive strain induced by the cage and parallels that of the bulk band gap as a function of hydrostatic pressure.

The current possibilities of *ab initio* calculations do not allow us to study the experimentally most studied zeolites with larger pores, where a more extensive cluster size dependence analysis could be performed. However, the study we have presented points out the relevance of the cage-cluster interaction in determining the equilibrium cluster structure. The equilibrium bond lengths can be substantially changed from their bulk value and lead to large energy shifts due to mechanical effects rather than to electronic confinement.

ACKNOWLEDGMENTS

The calculations have been performed at the Stichting Academisch Rekencentrum Amsterdam (SARA) within Grant No. SC-488 of the Stichting Nationale Computer Faciliteiten (NCF). Visualization of the structure has been performed using the graphical program MOLGEN developed by G. Schaftenaar at the CAOS/CAMM Center of Nijmegen. Partial financial support from MURST—Progetto “Fisica delle Nanostrutture”—is acknowledged. We are grateful to Professor A. Janner for his constructive criticisms.

¹See, e.g., P. M. Petroff, K. H. Schmidt, G. M. Ribeiro, A. Lorke, and J. Kotthaus, *Jpn. J. Appl. Phys., Part 1* **36**, 4068 (1997).

²For a review, see, e.g., *Inclusion Chemistry with Zeolites*, edited by N. Herron and D. R. Corbin (Kluwer, Dordrecht, 1995); J. A. Ozin, in *Materials Chemistry: An Emerging Discipline*, edited by L. V. Interrante, L. A. Casper, and A. B. Ellis, *Advances in Chemistry Series No. 245* (American Chemical Society, Washington, D.C., 1995), Chap. 14.

³J. E. Mac Dougall, H. Eckert, G. D. Stucky, N. Herron, Y. Wang, K. Moller, T. Bein, and D. Cox, *J. Am. Chem. Soc.* **111**, 8006 (1989); G. D. Stucky and J. E. Mc Dougall, *Science* **247**, 669 (1990).

⁴Y. Wang and N. Herron, *J. Phys. Chem.* **92**, 4988 (1988).

⁵K. L. Moran, T. E. Gier, W. T. A. Harrison, G. D. Stucky, H. Eckert, K. Eichele, and R. E. Wasylshen, *J. Am. Chem. Soc.* **115**, 10 553 (1993); K. L. Moran, *Chem. Mater.* **8**, 1930 (1996).

⁶A. Aparisi, V. Fornes, F. Marquez, R. Moreno, C. Lopez, and F. Meseguer, *Solid-State Electron.* **40**, 641 (1996).

⁷S. G. Romanov, N. P. Johnson, C. M. Sotomayor Torres, H. M. Yates, J. Agger, M. E. Pemble, M. W. Anderson, A. R. Peaker, and V. Butko, in *Proceedings of the Third International Symposium on Quantum Confinement: Physics and Applications*, edited by M. Cahay *et al.* (Electrochemical Society, Pennington, NJ, 1996).

⁸P. Armand, M. L. Saboungi, D. L. Price, L. Iton, C. Cramer, and M. Grimsditch, *Phys. Rev. Lett.* **79**, 2061 (1997).

⁹J. He, Y. Ba, C. I. Ratcliffe, J. A. Ripmeester, D. D. Klug, and J. S. Tse, *Appl. Phys. Lett.* **74**, 830 (1999).

¹⁰W. Chen, Z. Wang, Z. Lin, L. Lin, K. Fang, Y. Xu, M. Su, and J. Lin, *J. Appl. Phys.* **83**, 3811 (1998).

¹¹R. Car and M. Parrinello, *Phys. Rev. Lett.* **55**, 2471 (1985).

¹²F. Buda and A. Fasolino, *Phys. Rev. B* **52**, 5851 (1995).

¹³F. Filippone, F. Buda, S. Iarlori, G. Moretti, and P. Porta, *J. Phys. Chem.* **99**, 12 883 (1995).

¹⁴A. Trave, F. Buda, and A. Fasolino, *Phys. Rev. Lett.* **77**, 5405 (1996).

¹⁵A. Trave, F. Buda, and A. Selloni, *J. Phys. Chem. B* **102**, 1522 (1998).

¹⁶A. A. Demkov and O. F. Sankey, *Phys. Rev. B* **56**, 10 497 (1997).

¹⁷O. F. Sankey, A. A. Demkov, and T. Lenosky, *Phys. Rev. B* **57**, 15 129 (1998).

¹⁸See, e.g., R. G. Parr and W. Yang, *Density-Functional Theory of Atoms and Molecules* (Oxford University Press, New York, 1989); R. O. Jones and O. Gunnarson, *Rev. Mod. Phys.* **61**, 689 (1989).

¹⁹D. Vanderbilt, *Phys. Rev. B* **41**, 7892 (1990).

²⁰G. B. Bachelet, D. R. Hamann, and M. Schlüter, *Phys. Rev. B* **26**, 4199 (1982).

²¹G. Ortiz, Phys. Rev. B **45**, 11 328 (1992).

²²E. Hassan and H. D. Grundy, Acta Crystallogr., Sect. B: Struct. Sci. **B40**, 6 (1984).

²³F. Tassone, F. Mauri, and R. Car, Phys. Rev. B **50**, 10 561 (1994).

²⁴A. Fasolino, A. Shkrebtii, and A. Selloni, in *Physics of Solid Surfaces*, edited by G. Chiarotti, Landolt Börnstein, New Series,

Group III, Vol. 24, Pt. a (Springer-Verlag, Berlin, 1993), p. 125.

²⁵*Numerical Data and Functional Relationships in Science and Technology*, edited by O. Madelung, M. Schulz, and H. Weiss, Landolt-Börnstein, New Series, Group III, Vol. 17, Pt. a (Springer-Verlag, Berlin, 1982).